Stress Patterns Around Distal Angled Implants in the All-on-Four Concept Configuration

Tasneem Begg, BChD, BSc, MChD[1]/Greta A. V. M. Geerts, BChD, PDD, MChD[2]/
J. Gryzagoridis, PrEngBSc, MSc, PhD[3] [AU: Please supply given name of Dr Gryzagoridis.]

Purpose: *The All-on-Four concept advocates immediate loading and the placement of distal implants at an angle. The purpose of this study was to do a qualitative descriptive analysis of stress patterns around the distal angled implant of the All-on-Four concept.* ***Materials and Methods****: Four photoelastic acrylic resin models, each with 4 implants simulating the All-on-Four configuration, were prepared. The 2 central implants were placed vertically and parallel in each model, and the distal implant on each side was placed at an increasing angle (0, 15, 30, and 45 degrees) in each model. The 4 implants were splinted by means of a cast metal bar. The photoelastic models were placed between 2 parallel anvils. Pairs of abutments were systematically subjected to a load by suspending 5-, 10-, and 15-kg weights from one of the anvils. Photoelastic analysis was accomplished using a circular polariscope. The fringe patterns produced in the photoelastic resin for each implant and load were photographed with a digital camera. Fringe concentrations and the highest fringe order were recorded and described for the apical, central, and coronal regions of the distal angled implant for each load scenario.* ***Results:*** *For the implants placed at 15- and 30-degree angles, little difference in stress patterns was observed between the central straight implant and the distal angled implant. For every load scenario and for all angulations, the lowest fringe order was recorded at the central region of the implant. The highest fringe order for the apical region was always higher than the highest fringe order for the coronal region of the implant. Markedly increased isochromatic fringe concentrations were observed in model 4, which had the distal implants placed at a 45-degree angle.* ***Conclusion:*** *Peri-implant bone surrounding the 45-degree-angled distal abutment may be more prone to occlusal overload than bone surrounding implants with lesser tilts.* Int J Oral Maxillofac Implants 2009;24:xxx–xxx.

Key words: *angled implants, nonaxial loading, photoelastic analysis*

The rehabilitation of atrophied edentulous arches with endosseous implants in the posterior region is often complicated by the presence of anatomic structures such as the mandibular canal and maxillary sinus. In an effort to avoid these anatomic structures, transpose nerves, or graft the maxilla, distal implants may be tilted posteriorly 25 to 35 degrees from the axial.[1,2] As a result, implant-supported prostheses can be extended further distally and cantilever length can be reduced.[2–4] Maló et al introduced the All-on-Four concept for immediate loading of dental implants in the mandible, and later also in the maxilla. In this technique, a special surgical guide is used to place 2 parallel implants in the lateral incisor positions and a distal implant on each side just anterior to the mental foramen at a 30- to 45-degree angle.[5,6]

Occlusal forces are transmitted through the implant prosthesis to the peri-implant bone. It is difficult to quantify the magnitude and direction of occlusal forces.[7] But when occlusal forces exceed the mechanical or biologic load-bearing capacity of the implant or the prosthesis, causing a mechanical failure or loss of integration, they can be classified as overload.[7] Mechanical stress on bone results in strain.[7] The amount of strain is directly correlated to the stress applied to the bone and the stiffness of the bone. This means that the same force may affect different bone tissues differently.[7] Bone adapts its

[1]Private Practice, Bellville, South Africa.
[2]Senior Lecturer, Department of Restorative Dentistry, University of the Western Cape, Tygerberg, South Africa.
[3]Professor, Department of Mechanical Engineering, University of Cape Town, Rondebosch, South Africa.

Correspondence to: Prof G. A. V. M. Geerts, Department of Restorative Dentistry, University of the Western Cape, Private Bag XI, Tygerberg 7505, South Africa. Fax: +27-21-931-2287. Email: ggeerts@uwc.ac.za.

This paper was presented at the 41st meeting of the South African Division of the International Association for Dental Research, Pretoria, 6 September 2007.

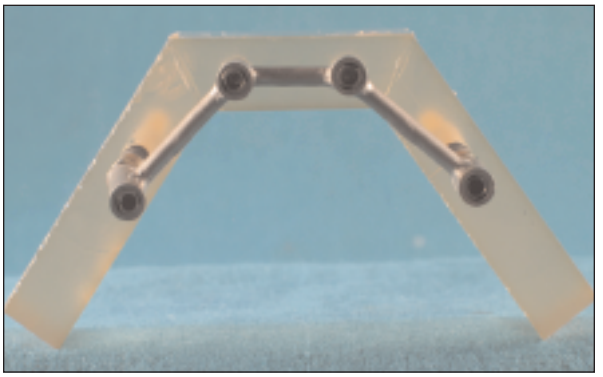

Fig 1a Top view of the photoelastic model showing the trapezoidal configuration of the implants connected with the bar.

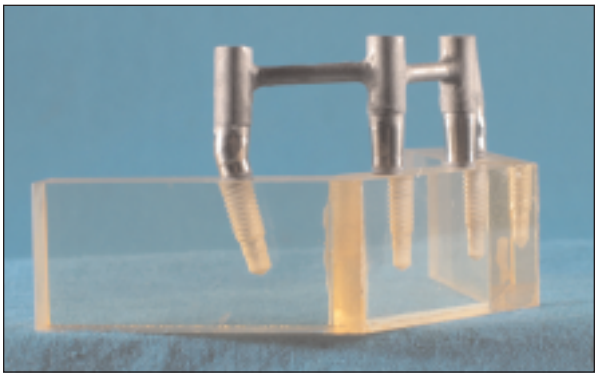

Fig 1b Side view of photoelastic resin model showing the angle of distal implant and indicating the 3 peri-implant zones: coronal = zone A, middle = zone B, and apical = zone C.

strength to the applied load.[8,9] If the strain goes beyond a threshold that exceeds the bone's capacity, fatigue fracture can occur.[8] Therefore, one must realize that it is not the load itself, but the effect of the load on bone that is important in implant dentistry.

Conflicting reports exist in the literature with regard to the effect of occlusal overloads on bone response. Results from animal studies show that occlusal overloading may cause peri-implant bone resorption if the forces exceed the physiologic tolerance of the alveolar bone.[10–13] Several clinical studies associate marginal bone loss around implants with high occlusal stress,[14–16] while others do not.[17,18]

Tilted implants and nonaxial loads are associated with higher stresses in peri-implant bone.[19–22] Nonaxial loading results in more dynamic remodeling of the surrounding bone; signs of osteoclastic activity were observed by Barbier and Schepers in an animal experiment.[23] Even if implants are placed perpendicular to the occlusal plane, forces of occlusion are rarely exclusively vertical.[24,25]

Osseointegration of immediately loaded implants has been proven successful, provided that loading forces and implant micromotion are controlled.[26] The purpose of this study was to describe the force-transfer characteristics for the distal implants, with increasing angulations (0 to 45 degrees), in a simulated All-on-Four configuration using photoelastic analysis. The hypothesis of this study is that increasing the angles of the distal implant in the All-in-Four configuration leads to higher strain production in the surrounding photoelastic material.

METHODS AND MATERIALS

Four identical models were constructed from photoelastic acrylic resin (Vishay, Malvern, PA). The models were 20 mm high and 10 mm wide. The lateral segments were 45 mm long, and the central anterior part was 35 mm long. For each model, implant sites were prepared with the aid of the All-On-Four surgical guide (Nobel Biocare, Göteborg, Sweden). All burs and tapping instruments used were from the Nobel Biocare Tapered surgical collection (Nobel Biocare). All implants (4.3 Replace Select, Nobel Biocare) were continually screwed in and out with an implant mount and a hand wrench until they could be fully seated with their 2-mm machined collar above the platform of the model. All implants were 13 mm long. In all models, the anterior implants were placed 15 mm apart, as measured between the center points of the implants. The distal implants were placed 20 mm from the center point of the anterior implants. In the first model, all implants were placed parallel to each other. In the remaining 3 models, the distal implants were tilted at 15-, 30-, and 45-degree angles, respectively (Figs 1a and 1b). Each implant was torqued to 35 Ncm. Straight 4-mm multiunit abutments (Nobel Biocare, Göteborg, Sweden) were connected to the parallel implants and 4-mm, 17-degree angled multiunit abutments were connected to the 15-degree angled implants and 30-degree multiunit abutments were connected to the 30- and 45-degree angled implants, respectively. All the abutments were torqued to 35 Ncm.

A 3-mm silicone spacer was constructed to mimic the gingival tissues. Multiunit abutment impression copings (Nobel Biocare) were connected and hand-tightened. Pickup impressions were made using a medium-consistency polyether impression material (Permadyne Penta Impression Material, 3M ESPE, St Paul, MN) in acrylic resin (Metroform, Metrodent, Huddersfield, United Kingdom) custom-made impression trays. Multiunit abutment laboratory analogues (Nobel Biocare) were attached to the impression copings, and casts were made in dental stone (Resin Rock, Whip Mix Corp, Louisville, KY). Provisional multiunit

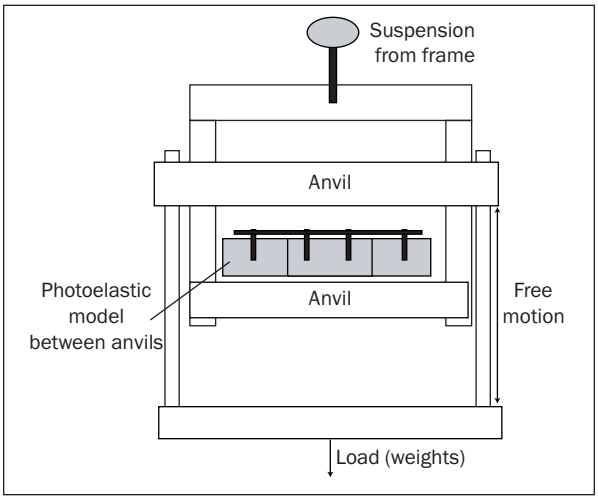

Fig 2 Setup of the photoelastic model positioned within the test apparatus.

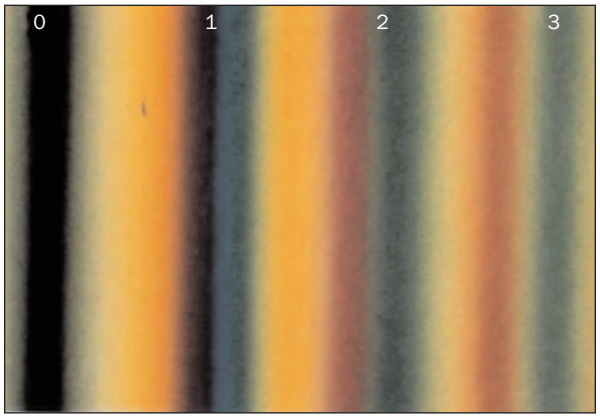

Fig 3 Isochromatic fringe characteristics. Fringe orders are indicated by numbers 0 to 3 (http://www.me.udel.edu[27]). **[AU: Please double check on URL (see query for Reference 27.]**

abutments were attached to each laboratory analogue. Five-millimeter-diameter hollow plastic sticks (Bego, Bremen, Germany) were milled out to 3.5 mm to create casting sleeves that were uniform in thickness (0.75 mm). The difference between the inside diameter of the sleeves (3.5 mm) and the size of the external connection of the abutment (3.3 mm) was 200 μm. This provided space for cement with a film thickness of 100 μm. A 2.5-mm-diameter solid plastic stick (Bego) was then cemented with instant cyanoacrylate adhesive (SuperGlue, Adlock, Johannesburg, South Africa) to each of the milled plastic sleeves. The plastic bars were sprued, invested, and cast (Tilite alloy, Talladium, Valencia, CA). The provisional abutments were covered with a thin layer of luting agent (Panavia F 2.0, Kuraray Medical Inc, Osaka, Japan) and slowly inserted into the finished cast bar. The bar was then placed on the photoelastic model and the abutments were torqued down to 15 Ncm.

Each photoelastic model was placed in a jig consisting of 2 parallel anvils and subjected to static compressive force by attaching a weight of 5, 10, and 15 kg (Fig 2). These weights represent loads of 49.05 N for the 5-kg weight, 98.06 N for the 10-kg weight, and 147.09 N for the 15-kg weight. **[AU: Please confirm that the numbers 49.05 N, 98.06 N, and 147.09 N are correct for the 3 scenarios; numbers differed in figures and different portions of the original text.]** The anvils compressed 2 adjacent abutments on the specimen for each individual load application: the left side implant together with the anterior left implant, the 2 central implants together, and the right side implant together with the anterior right implant. This was possible because the specimen could be rotated under the anvils to be normal to the illumination beam. Isochromatic fringes in the acrylic resin were photographed with a digital camera (Canon Powershot G3, Canon Inc, Tokyo, Japan) in the field of a circular polariscope. For examination of the fringes, the digital photographs were enlarged to 500% on a 17-inch computer monitor. The fringes were analyzed for 3 zones (A, B, and C), as shown in Fig 1b.

Figure 3 and Table 1 display the different colors and corresponding fringe order values produced by

Table 1 Relationship of Fringe Order to Relative Retardation[27]

Color	Approximate relative retardation		Fringe order no.
	nm	in ×106	
Black	0	0	0
Grey	160	6	0.28
White	260	10	0.45
Pale yellow	345	14	0.60
Orange	460	18	0.80
Dull red	520	20	0.90
Purple (tint of passage)	**575**	**22.7**	**1.00**
Deep blue	620	24	1.08
Blue-green	700	28	1.22
Green-yellow	800	32	1.39
Orange	935	37	1.63
Rose red	1,050	42	1.82
Purple (tint of passage)	**1,150**	**45.4**	**2.00**
Green	1,350	53	2.35
Green-yellow	1,440	57	2.50
Red	1,520	60	2.65
Red/green transition	**1,730**	**68**	**3.00**
Green	1,800	71	3.10
Pink	2,100	83	3.65
Pink/green	**2,300**	**90.8**	**4.00**
Green	2,400	95	4.15

[AU: What is meant by the bolded text in Table 1?]

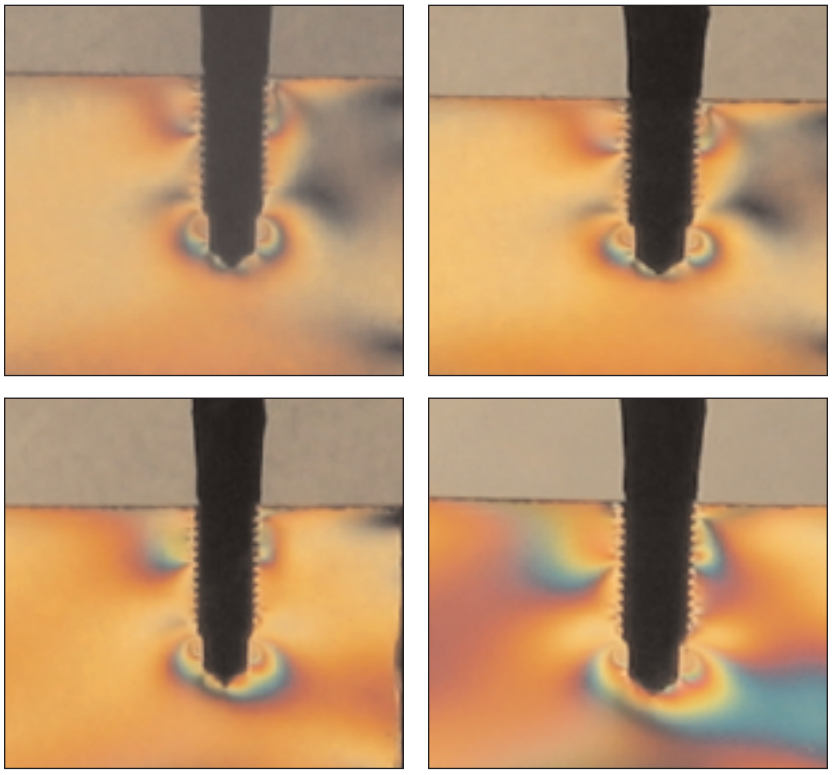

Fig 4 Distal implant on right side of model 1 (all implants parallel). a = unloaded; b = loaded with 49.05 N; c = loaded with 98.06 N; **[AU: 98.06 correct, rather than 47.09 N?]** d = loaded with 147.09N.

2-dimensional photoelastic material.[27] The following paragraph, adapted from www.me.udel.edu,[27] explains the interpretation of the color fringes:

> An unloaded photoelastic model observed with a polariscope appears black. As a load is gradually applied, the stressed region begins to take on color—first a gray, then white, violet, yellow, blue, orange, green, red, yellow, purple, orange, and a deep blue. The purple fringe, which is easily distinguished from the red and blue on either side and is very sensitive to a small change in strain level, is referred to as the *tint of passage*. Because of its distinctiveness and resolution, the purple tint of passage is selected to mark the increment in relative retardation equal to a fringe order of unity ($N = 1$). Subsequent recurrence of the tint of passage with greater relative retardation signifies the presence of higher fringe orders ($N = 2$, $N = 3$, etc.) Once one fringe has been identified, orders can be assigned to the other fringes, making certain that the direction of increasing fringe order corresponds to the correct color sequence. By this process the observer can locate the highest fringe orders and the most highly strained regions. Areas of closely spaced fine fringes attract the observer's attention: steep strain gradients signify high strains. Large areas where the pattern is almost uniformly black or gray usually indicate an understressed region.[27p?] **[AU: Please provide page number of quoted material.]**

Two factors were considered in the analysis: (*1*) the number of fringes and (*2*) the proximity of fringes to each other. The number of fringes indicates strain magnitudes. If fringes are close together, stress concentrations are high. The stress intensity, indicated by the number of fringes and its location, was compared for each of the photoelastic models.

RESULTS

The following paragraphs describe the color fringe patterns for each model, based on the information supplied in Table 1 and Fig 3. The isochromatic fringe patterns and fringe orders generated around the distal implants for each model are shown in Figs 4 to 7. Generally, for all distal implants and for each load, the fringe order was higher in zone C than in zone A. The lowest fringe orders were observed for zone B (Table 2). **[AU: OK to cite Table 2 here? It was not cited otherwise.]**

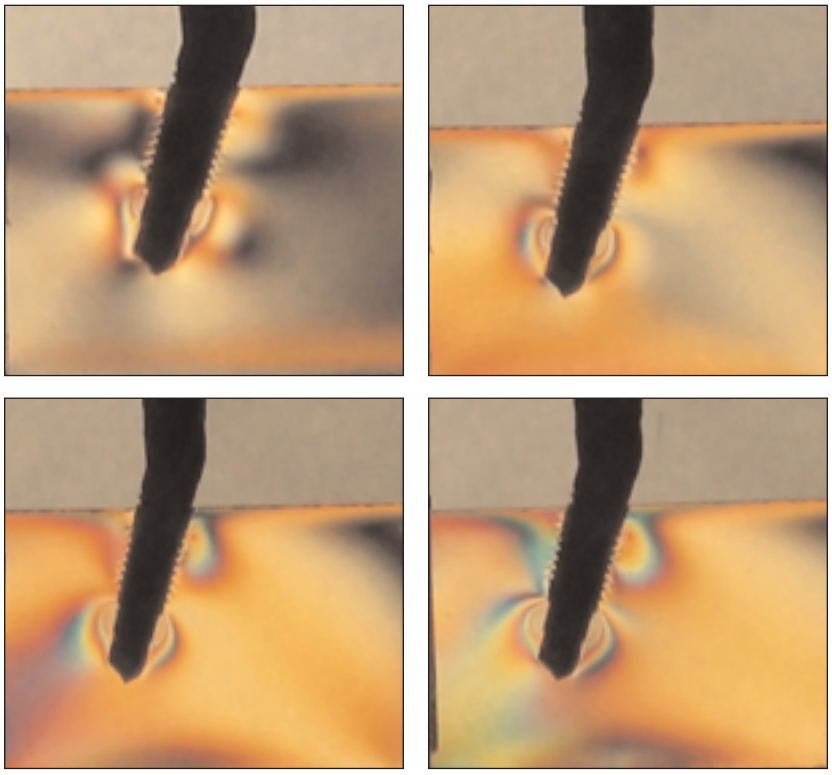

Fig 5 Distal implant placed at 15-degree angle on left side of model 2. a = unloaded; b = loaded with 49.05 N; c = loaded with 98.06 N; d = loaded with 147.09 N.

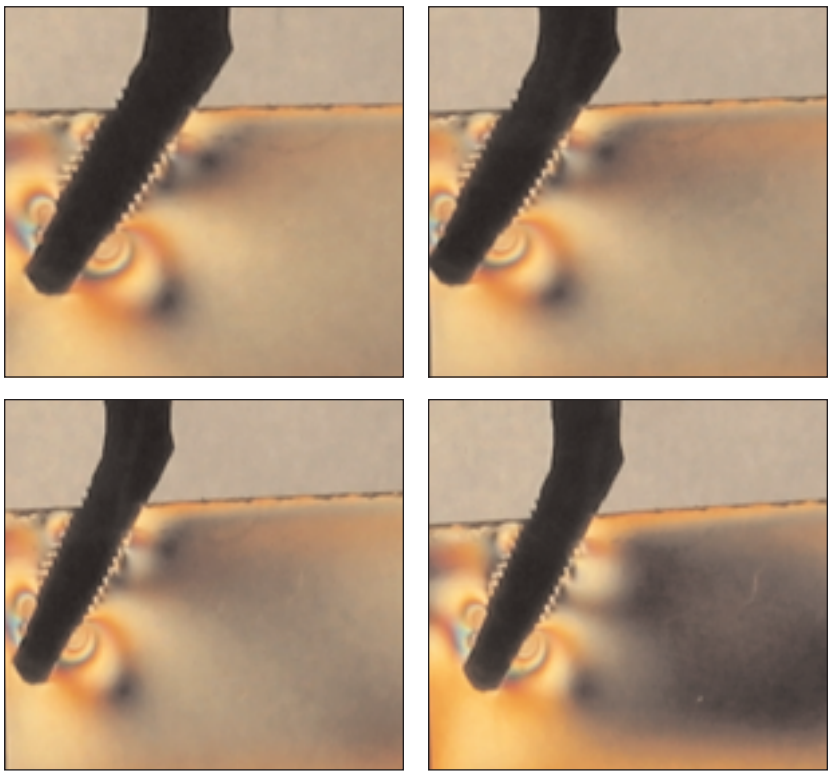

Fig 6 Distal implant placed at 30-degree angle on left side of model 3. a = unloaded; b = loaded with 49.05 N; c = loaded with 98.06 N; d = loaded with 147.09 N.

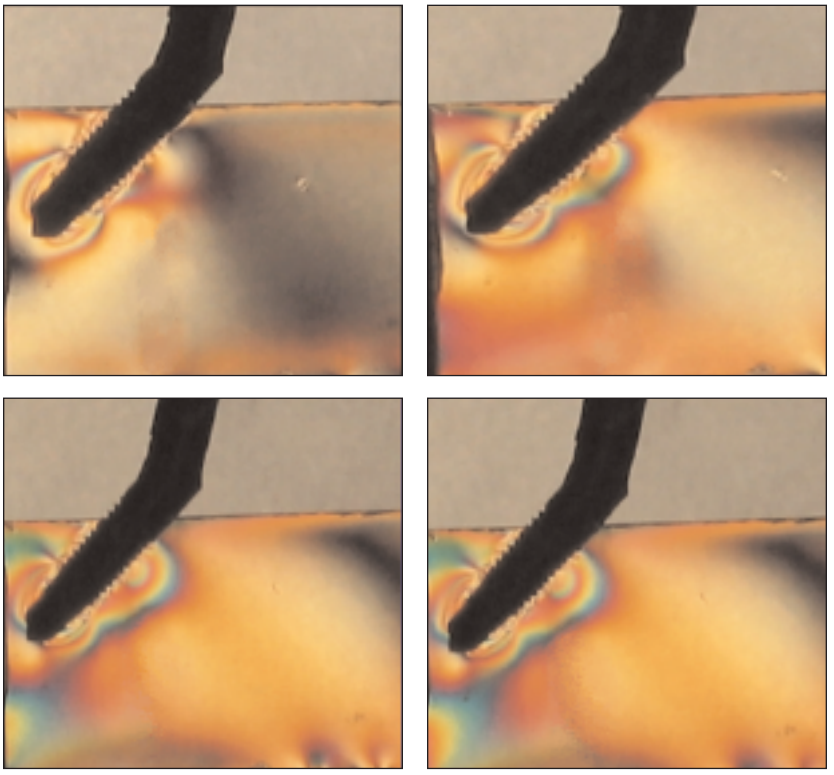

Fig 7 Distal implant placed at 45-degree angle on left side of model 4. a = unloaded; b = loaded with 49.05 N; c = loaded with 98.06 N; d = loaded with 147.09 N.

Table 2 Highest Fringe Orders for Zones A, B, and C of the Distal Implants

	Model 1			Model 2			Model 3			Model 4		
Load	A	B	C	A	B	C	A	B	C	A	B	C
0 kg/0 N	1.08	0.60	1.63	0.90	0.60	1.63	0.90	0.60	1.63	0.60	0.80	1.82
5 kg/49.05 N	1.39	0.60	1.63	1.00	0.60	1.82	1.00	0.60	1.63	1.39	1.82	2.00
10 kg/98.06 N	1.39	0.80	1.82	1.63	0.80	2.65	1.22	0.60	1.63	1.82	1.82	2.65
15 kg/147.09 N	1.63	1.00	2.65	1.82	1.63	2.65	1.39	0.60	1.63	2.00	1.82	3.10

For each load, the fringe patterns and orders around the distal implants were similar on both sides, except for model 2. For model 2, the right side implant showed a lack of fringe patterns for all loads.

For model 1, the central implants showed distinct symmetric fringe concentrations in zones A and C. Little change in fringe order concentrations was observed with increasing loads.

The distal implant on the right side (Fig 4) showed an increase in fringe order concentrations in zones A, B, and C with increasing loads. With the 5-kg weight (49.05-N load), fringe concentrations were symmetric and within the first fringe order. Zone A showed a dull red/purple color (1.0) on the distal side and green/yellow (1.39) on the mesial side. Zone C depicted concentrations within the second fringe order (1.63) in orange. With a 10-kg weight (98.06-N load), an increase in fringe order (1.82) was noted as indicated by the red/purple color in zone C. With the 15-kg weight (147.09-N load) the fringe concentrations became asymmetric in zones A and C. In zone A the fringe concentrations increased (2.00), as indicated by a faint purple shade. In zone C fringe concentrations reached the third fringe order (2.65), represented by a faint red shade. The fringe concentrations on the left hand side were not identical to those seen for the right-side implant; however, the pattern was similar.

Unloaded, the left distal implant on model 2 (Fig 5) displayed pale yellow and black shades for zones A and B, respectively. Zone C showed ill-defined stress concentrations, indicated by pale blue/green shades. With a 5-kg weight (49.05-N load), zone A displayed fringe concentrations with an orange tint (0.80) on the mesial aspect and a dull red shade (0.90) on the distal side. In zone B only pale yellow shades (0.60) could be seen. In zone C the fringe concentrations displayed were rose/red in color (1.82), changing to orange distally (1.63). With the 10-kg

weight (98.06-N load) there was an increase in fringe concentrations along the entire length of the implant. Zone A had fringe concentrations on the distal aspect of the implant within the second fringe order indicated by the orange color (1.63). In zone B a pale yellow shade (0.60) was seen and on the mesial aspect an orange shade was observed within the first fringe order (0.80). In zone C, a red tint (2.65) was displayed. With the 15-kg weight (147.09-N load) enlarged areas of stress patterns were observed along the length of the implant. In zone A, a rose/red color (1.82) was seen, and distally an orange tint (1.63) was noted. In zone B a blue/green spectrum (1.22) was observed, with orange distally (1.63). There was an increase from second to third fringe orders in zone C, indicated by a red shade (2.65). For the right-hand distal implant, the fringe configurations were similar, albeit of a slightly lower order.

For model 3, the unloaded left-side implant (Fig 6) demonstrated residual fringe concentrations in zones A and C. The stress magnitude in zone A was minimal, indicated by an orange hue (0.80) with a faint dull red (0.90) fringe. Zone C had an orange band closest to the apex of the implant (1.63). With increasing loads, the fringe concentrations remained the same and enlarged slightly. The unloaded picture displayed a grey/pale yellow shade in the far fields. With the 15-kg weight (147.09-N load) the stress concentration patterns intensified close to the implant body and the far field area changed to black.

For model 4, with the unloaded distal implant, fringe concentrations were observed distally in zone B and surrounding the apex in zone C (Fig 7). For all zones, the magnitude of stress concentrations increased gradually with an increase in load. For zone A, there was a clear difference in pattern between the mesial and distal sides of the implant, with the distal side showing more fringes. For zone C, the pattern was symmetric for the mesial and distal sides. The 15-kg weight (147.09-N load) resulted in fringe concentrations along the entire length of the implant, with the highest stress of a magnitude 3.10, with the green shade close to the apex of the implant.

DISCUSSION

Photoelasticity is a whole field technique, which provides information of principal stress difference and the orientation of principal stress at a point of interest in a 2-dimensional model. A strain field cannot be measured. The models used in the paper characterized only the loading situation of the implant support because of the different angles of the implants. Fringes that become visible in photoelastic models cannot be quantitatively interpreted because they are caused by the passage of light through varying stress fields over different path lengths. A solution to this problem is the very expensive frozen stress method, which was not used for the present study. Thus, only a qualitative interpretation of the fringes can be made here.

Marginal bone loss around implants has been associated with overloading, leading to excessive stress and strain gradients in peri-implant bone.[16] Tilted implants and nonaxial loads are associated with higher stresses in peri-implant bone.[19–21] An offset location for splinted implants could reduce stress but does not necessarily compensate for the higher strains caused by nonaxial loading.[22] The All-on-Four principle recommends the placement of angled distal implants to avoid anatomic structures and limit cantilever length. This results in nonaxial loading of the distal implant and could create higher stress areas in the peri-implant bone. This study analyzed the photoelastic strain patterns surrounding distal implants placed at 0-, 15-, 30-, and 45-degree angles.

In model 1 (Fig 4), all implants were placed parallel. Fringe concentrations were found in the coronal and apical zones of all 4 parallel implants. This stress pattern supports previous findings.[22] The fringe order and magnitude of stress patterns increased proportionally to the increases in loading.

In model 2 (Fig 5), the distal implants were placed at a 15-degree angle. The left distal implant showed an increase in fringe patterns with increasing load applications. The strains in zones A and C were always higher than the strain in zone B. This also corresponds to the classically reported stress patterns around implants.[26] Strains were highest in zone C for each load. The fringe concentrations observed around the right distal implant were unexpected and differed from those seen around the left distal implant. There appeared to be no force transfer from the implant to the photoelastic model. A possible explanation is that the load applied above the implant was diffused or distributed to the rest of the implants via the connecting bar, or that the implant/model interface was deficient.

In model 3 (Fig 6), the distal implants were placed at a 30-degree angle. With increasing loads, there was a proportional increase in fringe patterns in zone C for each implant. There was no difference in the isochromatic stress concentrations between the straight and angled implants.

In model 4 (Fig 7), the distal implants were placed at a 45-degree angle. There were clearly higher isochromatic fringe concentrations around the angled implants than around the straight implants of

model 1. The fringe concentration at the apex of the angled implants in the 15-kg weight scenario (147.09-N load) was the highest of all the fringe concentrations observed in this study.

In each model, higher loads resulted in equal or higher fringe concentrations in zones A and C of the distal angled implants. In comparing the different angled implants across the models for the 15-kg weight (147.09-N load) scenario, there was no remarkable difference in strain magnitude between models 1, 2, and 3. However, there was a dramatic increase in strain pattern for the 45-degree-angled implants of model 4.

The All-on-Four concept advocates immediate loading. A slight load on healing bone shortens healing time rather than prolonging it.[7] On the other hand, overloading and fracturing happen more readily in healing bone than in normal bone.[8] Occlusal loading in the period immediately after placement may be sufficient to cause microdamage in bone surrounding the implant, even though the same load will not do so after healing and adaptation of the bone around the implant.[7] **[AU: Previous sentence edited correctly?]** Immediately loaded implants osseointegrate, provided that forces and implant micromotion are controlled.[26] With increasing loads, a marked increase in fringe patterns was observed surrounding the 45-degree distal abutment compared to the lesser angles. Within the context of immediate loading, it might be recommended to avoid the higher angles for the distal implants of the All-on-Four configuration to minimize forces on vulnerable healing bone.

For the sake of standardization within this study, the same length of implants was used for all angles. However, clinically, because of the angle of the distal implants in the All-on-Four concept, longer implants can be selected for this position than if they were to be placed in a vertical position. Furthermore, more failures have been observed with shorter implants.[16] The longer distal implant is to be recommended if an angle of 45 degrees is used, because in this study the authors observed a drastic increase in fringe concentrations for this angle.

The present study used one type of implant. Therefore, the results may not necessarily be applicable to implants with different shapes and surface topographies. This is a study limitation.

The photoelastic model is a homogenous medium and does not imitate the different properties of cancellous and cortical bone. Many studies have observed an increased rate of late failure for implants placed in areas of low bone density, ie, posteriorly or in the maxilla.[7] Since the highest fringe concentrations were observed in zone A (coronal area) and zone C (apical area) for all loads, and a particularly high increase was seen in fringe concentrations for the 15-kg weight (147.09-N load) for the 45-degree-angle implant, it is speculated that in areas of poor bone quality, these areas are at a higher risk of overloading. It is interesting to note that, for each load application and for each angulation, the highest fringe order recorded in zone A was always lower than the highest fringe order in zone C. However, overload is associated with marginal bone loss and not apical bone loss. Zone B always had the lowest fringe order.

The implants were torqued in the photoelastic resin models. The same type of anchorage does not exist in real trabecular bone with lower elastic properties as cortical bone. Further, the implants in the models represent a bone implant situation without osseointegration.

The hypothesis of this in vitro study was that increasing angles of the distal implant in the All-in-Four configuration lead to higher strain production in the surrounding photoelastic material. Within the limitations of this study, the hypothesis can be supported for the 45-degree-angled implant, but not for the lesser angles.

CONCUSIONS

In the All-on-Four configuration, markedly higher fringe orders around the 45-degree-angled distal implant were observed in this study. These fringe orders also increased with increasing load application. This means that the 45-degree-angled implant may produce more strain in peri-implant tissues. Long-term prospective clinical studies should be performed to establish the clinical significance of these in vitro findings.

ACKNOWLEDGMENT

The authors thank Nobel Biocare for supplying the implant components.

REFERENCES

1. Ten Bruggenkate CM, Sutter F, Oosterbeek HS, Schroeder A. Indications for angled implants. J Prosthet Dent 1992;67:85–93.
2. Krekmanov L, Kahn M, Rangert B, Lindstrom H. Tilting of posterior mandibular and maxillary implants for improved prosthesis support. Int J Oral Maxillofac Implants 2000;15:405–414.
3. Aparicio C, Perales P, Rangert B. Tilted implants as an alternative to maxillary sinus grafting: A clinical, radiologic, and periotest study. Clin Implant Dent Relat Res 2001;3:39–49.

4. Kronstrom M, Widbom T, Lofquist LE, Henningson C, Widbom C, Lundberg T. Early functional loading of conical Brånemark implants in the edentulous mandible: A 12-month follow-up clinical report. J Prosthet Dent 2003;89:335–340.
5. Maló P, Rangert B, Nobre M. "All-on-Four" immediate-function concept with Brånemark System implants for completely edentulous mandibles: A retrospective clinical study. Clin Implant Dent Relat Res 2003;5(suppl 1):2–9.
6. Maló P, Rangert B, Nobre M. All-on-4 immediate-function concept with Brånemark System implants for completely edentulous maxillae: A 1-year retrospective clinical study. Clin Implant Dent Relat Res 2005;7(suppl 1):S88–94.
7. Isidor F. Influence of forces on peri-implant bone. Clin Oral Implants Res 2006;17(suppl 2):8–18.
8. Frost HM. Perspectives: Bone's mechanical usage windows. Bone Miner 1992;9:257–271.
9. Frost HM. A 2003 update of bone physiology and Wolff's Law for clinicians. Angle Orthod 2004;74:3–15.
10. Isidor F. Loss of osseointegration caused by occlusal load of oral implants. A clinical and radiographic study in monkeys. Clin Oral Implants Res 1996;7:143–152.
11. Miyata T, Kobayashi Y, Araki H, Ohto T, Shin K. The influence of controlled occlusal overload on peri-implant tissue. Part 3: A histologic study in monkeys. Int J Oral Maxillofac Implants 2000;15:425–431.
12. Duyck J, Ronold HJ, Van Oosterwyck H, Naert I, Vander Sloten J, Ellingsen JE. The influence of static and dynamic loading on marginal bone reactions around osseointegrated implants: An animal experimental study. Clin Oral Implants Res 2001;12:207–218.
13. Melsen B, Lang NP. Biological reactions of alveolar bone to orthodontic loading of oral implants. Clin Oral Implants Res 2001;12:144–152.
14. Naert I, Quirynen M, van Steenberghe D, Darius P. A study of 589 consecutive implants supporting complete fixed prostheses. Part II: Prosthetic aspects. J Prosthet Dent 1992;68:949–956.
15. Naert IE, Duyck JA, Hosny MM, Quirynen M, van Steenberghe D. Freestanding and tooth-implant connected prostheses in the treatment of partially edentulous patients Part II: An up to 15-years radiographic evaluation. Clin Oral Implants Res 2001;12:245–251.
16. Quirynen M, Naert I, van Steenberghe D. Fixture design and overload influence marginal bone loss and fixture success in the Brånemark system. Clin Oral Implants Res 1992;3:104–111.
17. Engel E, Gomez-Roman G, Axmann-Krcmar D. Effect of occlusal wear on bone loss and Periotest value of dental implants. Int J Prosthodont 2001;14:444–450.
18. Wennerberg A, Carlsson GE, Jemt T. Influence of occlusal factors on treatment outcome: A study of 109 consecutive patients with mandibular implant-supported fixed prostheses opposing maxillary complete dentures. Int J Prosthodont 2001;14:550–555.
19. Canay S, Hersek N, Akpinar I, Asik Z. Comparison of stress distribution around vertical and angled implants with finite-element analysis. Quintessence Int 1996;27:591–598.
20. Ueda C, Markarian RA, Sendyk CL, Lagana DC. Photoelastic analysis of stress distribution on parallel and angled implants after installation of fixed prostheses. Braz Oral Res 2004;18:45–52.
21. Kitamura E, Stegaroiu R, Nomura S, Miyakawa O. Influence of marginal bone resorption on stress around an implant—A three-dimensional finite element analysis. J Oral Rehabil 2005;32:279–286.
22. Sütpideler M, Eckert SE, Zobitz M, An KN. Finite element analysis of effect of prosthesis height, angle of force application, and implant offset on supporting bone. Int J Oral Maxillofac Implants 2004;19:819–825.
23. Barbier L, Schepers E. Adaptive bone remodeling around oral implants under axial and nonaxial loading conditions in the dog mandible. Int J Oral Maxillofac Implants 1997;12:215–223.
24. Rangert B, Jemt T, Jorneus L. Forces and moments on Brånemark implants. Int J Oral Maxillofac Implants 1989;4:241–247.
25. Sahin S, Cehreli MC, Yalcin E. The influence of functional forces on the biomechanics of implant-supported prostheses—A review. J Dent 2002;30:271–282.
26. Duyck J, Vandamme K, Geris L, et al. The influence of micromotion on the tissue differentiation around immediately loaded cylindrical turned titanium implants. Arch Oral Biol. 2006;51:1-9.
27. http://www.me.udel.edu/meeg215/MEEG_215_Lab3_07.pdf; 3–4. Accessed 25 September 2008. **[AU: This link no longer works. Please find a new link that is operational. Also, please supply a title, authors, and date of publication. (Has this document been published in a peer-reviewed journal? If so, please supply complete publication information.)]**